

Adaptation and the evolution of parasite virulence in a connected world

Geoff Wild[†], Andy Gardner[‡] & Stuart A. West^{†*}

[†]*Department of Applied Mathematics, University of Western Ontario, London, Ontario N6A 5B7, Canada*

[‡]*Institute of Evolutionary Biology, University of Edinburgh, King's Buildings, Edinburgh EH9 3JT, UK*

^{*}*Present address: Department of Zoology, University of Oxford, Oxford, OX1 3PS, UK*

Supplementary Information

Patch Dynamics

Habitat patches, in our model, are classified according the number of susceptible hosts (i) and the number of infected hosts (j) found to reside there (here, $0 \leq i + j \leq N$). We use the vector, (i, j) to indicate the class to which a given patch belongs.

Let $x_{(i,j)}$ denote the density of class- (i,j) patches in our infinite model population, and let $p_{(i,j)} = x_{(i,j)} / \sum_{(k,l)} x_{(k,l)}$ denote the population-wide frequency of class- (i, j) patches.

Class- (i,j) patches are created from other patches, whose classification belongs to the set

$$\mathbf{U}_{(i,j)} = \{(i-1, j), (i+1, j), (i, j+1), (i+1, j-1)\}$$

as hosts either die or become infected. Class- (i,j) patches are destroyed in the same way to become patches whose classification belongs to the set

$$\mathbf{D}_{(i,j)} = \{(i-1,j), (i+1,j), (i,j-1), (i,j+1)\}.$$

If $q_{(i,j),(k,l)}$ denotes the rate at which a class- (k,l) patch becomes a class- (i,j) patch, then the *patch dynamics*, are described by

$$\frac{dx_{(i,j)}}{dt} = \sum_{(k,l) \in \mathbf{U}_{(i,j)}} q_{(i,j),(k,l)} x_{(k,l)} - \sum_{(k,l) \in \mathbf{D}_{(i,j)}} q_{(k,l),(i,j)} x_{(i,j)}. \quad (\text{S1})$$

In Table S1, we state the rates $q_{(i,j),(k,l)}$, using the notation introduced in the main text of the paper, as well as the shorthand notation,

$$b_{(k,l)} = \begin{cases} b(1-d_h)(k+l) + bd_h(S+I) & \text{for } k+l < N \\ 0 & \text{otherwise} \end{cases}$$

where b is the per capita rate of host reproduction (for both susceptible and infected hosts), d_h is the natal dispersal rate of the host, and

$$S = \sum_{(k,l)} kp_{(k,l)} = \sum_{k=0}^N \sum_{l=0}^{N-k} kp_{(k,l)},$$

$$I = \sum_{(k,l)} lp_{(k,l)} = \sum_{k=0}^N \sum_{l=1}^{N-k} lp_{(k,l)} = \sum_{k=0}^N \sum_{l=0}^{N-k} lp_{(k,l)}.$$

Additional shorthand notation includes,

$$\beta_{(k,l)}(z) = \beta(z) \left[(1-d_p)l + d_p I \right] k,$$

and

$$\tilde{\beta}_{(k,l)}(z) = \begin{cases} \beta(z) d_p (k+1) p_{(k+1,l-1)} & k+l \leq N, \\ 0 & \text{otherwise.} \end{cases}$$

Since $\sum_{(i,j)} dx_{(i,j)}/dt = 0$ (patches are neither created, nor destroyed) we can say that

$$\frac{dp_{(i,j)}}{dt} = \sum_{(k,l) \in \mathbf{U}_{(i,j)}} q_{(i,j),(k,l)} p_{(k,l)} - \sum_{(k,l) \in \mathbf{D}_{(i,j)}} q_{(k,l),(i,j)} p_{(i,j)}. \quad (\text{S2})$$

The inclusive fitness analysis we undertake in the next section (and, indeed, in the main text) assumes that the solution of equation (S2) tends toward a unique, globally stable equilibrium. From this point forward, then, $\mathbf{p} = (p_{(i,j)})_{(i,j)}$ will refer only to this equilibrium state. We suppose further that classes (i,j) such that $j \geq 1$ are in the support of \mathbf{p} . Unfortunately, non-trivial equilibrium solutions of equation (S1) can only be found by numerical methods. Nevertheless, numerical investigation indicates that our assumption, above, holds for a wide range of parameter values.

Inclusive Fitness Model

In this section, we give a more detailed description of how we reach equation (1) of the main text. The approach is the same as that used recently by Alizon & Taylor³¹ (see also Appendix A of ref. 32). We begin by assuming a monomorphic parasite population, i.e. a parasite population in which all individuals employ the same virulence “strategy” z .

Both the class to which a parasite belongs, and the distribution of the different patch types in the population have important implications for parasite fitness. Let $w_{(i,j),(k,l)}$ denote the (i,j) fitness of class- (k,l) parasite, defined as the per capita rate at which class- (k,l) pathogens produce class- (i,j) infections, when the distribution of patch types has reached an equilibrium—one that includes patches with infected individuals. Expressions for $w_{(i,j),(k,l)}$ are summarized in Table S2. From these “fitness functions” we can determine $u_{(i,j)}$, the equilibrium frequency of class- (i,j) parasites, as well as $v_{(i,j)}$ the individual reproductive value of class- (i,j) parasites (i.e. the per capita contribution of class- (i,j) to the generations in the distant future). The former quantities satisfy the equation, $\sum_{(k,l)} w_{(i,j),(k,l)} u_{(k,l)} = 0$, whereas the latter quantities satisfy, $\sum_{(i,j)} v_{(i,j)} w_{(i,j),(k,l)} = 0$.

Equilibrium frequencies and reproductive values, as we will see, are some of the key building blocks of kin selection models^{32, 33}.

We have, so far, been thinking of a scenario in which all parasites exploit hosts to the same extent. In this scenario, all infected hosts suffer “normal” disease-induced mortality at rate, z . To build our kin selection model, we introduce slightly deviant and extremely rare exploitation strategy that changes the mortality rate of infected hosts by a very small amount^{34,35}. We then ask, does a shift from a normal host exploitation strategy to a deviant one increase or decrease the inclusive fitness of a parasite?

Let $\Delta W_{(k,l)}$ denote the change that occurs in the inclusive fitness of a single class- (k,l) pathogen (the “focal actor”) as it changes its exploitation strategy from normal to deviant. As mentioned above, the strategy shift implies that the mortality of the individual playing host to the focal actor changes by a small amount, which we now denote as, $\delta > 0$. We record this increased mortality as a cost paid by the focal actor and each of its $(l - 1)$ patchmates, writing $-\delta v_{(k,l)}(1 + (l - 1)r_{(k,l)}) = -\delta v_{(k,l)}\bar{r}_{(k,l)}l$, where $r_{(k,l)}$ is the relatedness between two different parasites on the same class- (k,l) patch, and $\bar{r}_{(k,l)}$ is the relatedness between two pathogens on the same class- (k,l) patch, chosen at random with replacement. The term $v_{(k,l)}$ reflects the fact that the costs are in (k,l) -fitness and must be included to make sure all fitness changes receive proper weighting in the final calculation.

Increased host mortality also carries with it certain inclusive fitness benefits when $l > 1$. When the focal actor and its host have died, $(l - 1)$ surviving parasites immediately join class- $(k, l - 1)$. We record this change as, $\delta v_{(k,l-1)}r_{(k,l)}(l - 1) = \delta v_{(k,l-1)}(\bar{r}_{(k,l)}l - 1)$.

When $k \geq 1$ susceptible hosts can be found locally, and so increased host exploitation implies that the focal actor produces new local infections at a higher rate. In this case, the rate at which local infections occur is increased by $\delta\beta'(z)(1 - d_p)k$. We record the inclusive-fitness change as $\delta v_{(k-1,l+1)}\beta'(z)(1 - d_p)k(1 + \bar{r}_{(k,l)}l)$. The multiplier, $(1 + \bar{r}_{(k,l)}l)$ is included here, because, when a new local infection occurs, the actor, the

actor's "offspring" and the actor's $(l - 1)$ patchmates all become class- $(k-1, l+1)$ parasites simultaneously. Naturally, when the actor and its patchmates become class- $(k-1, l+1)$ parasites they cease to be class- (k, l) pathogens, hence we must record an additional inclusive fitness loss of, $-\delta v_{(k,l)} \beta'(z) (1 - d_p) k l \bar{r}_{(k,l)}$ in our calculation.

Increased host exploitation also means that the rate at which the focal parasite produces non-local infections increases. Specifically, if $p_{(i+1,j-1)}$ denotes the frequency of class- $(i+1, j-1)$ patches, the increase in $w_{(i,j)}$ is given by, $\delta v_{(i,j)} \beta'(z) d_p (i+1) p_{(i+1,j-1)}$. We make the standard assumption that non-local infections occur only on very distant patches, so that the effects these infections have on the fitness of (similarly distant) relatives of the focal parasite need not be included in our calculation. We can then write the change in the inclusive fitness of a class- (k, l) parasite as

$$\begin{aligned} \Delta W_{(k,l)} = & -\delta v_{(k,l)} \bar{r}_{(k,l)} l + \delta v_{(k,l-1)} (\bar{r}_{(k,l)} l - 1) + \delta v_{(k-1,l+1)} \beta'(z) (1 - d_p) k (1 + \bar{r}_{(k,l)} l) \\ & - \delta v_{(k,l)} \beta'(z) (1 - d_p) k l \bar{r}_{(k,l)} + \delta \sum_{(i,j)} v_{(i,j)} \beta'(z) d_p (i+1) p_{(i+1,j-1)} \end{aligned} \quad (S3)$$

which rearranges to give equation (1) of the main text. The overall change in the inclusive fitness of the mutant, call it ΔW , is a weighted average of all $\Delta W_{(k,l)}$, where class frequencies $u_{(k,l)}$ are used as weights.

Calculation of Relatedness Coefficients

We can calculate the coefficients of relatedness for a neutral population using the notion of identity by descent, or IBD. Two genes are said to be IBD provided they have descended from a common ancestor without intervening mutation. The coefficient of consanguinity (CC) between two (same-locus) genes is simply the probability that the alleles are IBD.

Let $r_{(i,j)}$ with $j \geq 2$ denote the CC between genes drawn from two different class- (i, j) parasites found on the same patch. To calculate $r_{(i,j)}$, observe that a class- (i, j) patch was a class- (k, l) patch dt time units ago with probability $\alpha_{(i,j),(k,l)}dt$, where $\alpha_{(i,j),(k,l)} = \frac{q_{(i,j),(k,l)}P_{(k,l)}}{P_{(i,j)}}$. We use $\alpha_{(i,j),(k,l)}$ to write a differential equation that describes how the CCs $r_{(i,j)}$ change over time. Assuming $j > 2$, then

$$\begin{aligned} \frac{dr_{(i,j)}}{dt} = & \alpha_{(i,j),(i-1,j)}(r_{(i-1,j)} - r_{(i,j)}) + \alpha_{(i,j),(i+1,j)}(r_{(i+1,j)} - r_{(i,j)}) + \alpha_{(i,j),(i,j+1)}(r_{(i,j+1)} - r_{(i,j)}) \\ & + \alpha_{(i,j),(i+1,j-1)} \frac{(1-d_p)(j-1)}{(1-d_p)(j-1) + d_p I} \left[\frac{2}{j(j-1)} + \left(1 - \frac{2}{j(j-1)}\right) r_{(i+1,j-1)} - r_{(i,j)} \right] \\ & + \alpha_{(i,j),(i+1,j-1)} \frac{d_p I}{(1-d_p)(j-1) + d_p I} \left[\left(1 - \frac{2}{j}\right) r_{(i+1,j-1)} - r_{(i,j)} \right]. \end{aligned} \quad (\text{S4})$$

We omit the term $\alpha_{(i,j),(i-1,j)}(r_{(i-1,j)} - r_{(i,j)})$ in (S4) when $i = 0$, and we omit the terms $\alpha_{(i,j),(i+1,j)}(r_{(i+1,j)} - r_{(i,j)})$ and $\alpha_{(i,j),(i,j+1)}(r_{(i,j+1)} - r_{(i,j)})$ when $i + j = N$. When $j = 2$, there are no terms in eqn (A6) that involve the undefined coefficient $r_{(i+1,j-1)}$. In this case, (S4) becomes

$$\begin{aligned} \frac{dr_{(i,2)}}{dt} = & \alpha_{(i,2),(i-1,2)}(r_{(i-1,2)} - r_{(i,2)}) + \alpha_{(i,2),(i+1,2)}(r_{(i+1,2)} - r_{(i,2)}) + \alpha_{(i,2),(i,3)}(r_{(i,3)} - r_{(i,2)}) \\ & + \alpha_{(i,2),(i+1,1)} \left[\frac{(1-d_p)}{(1-d_p) + d_p I} - r_{(i,2)} \right]. \end{aligned}$$

Remarkably, at equilibrium $r_{(i,j)} = r$ for all (i, j) , where

$$r = \frac{(1-d_p)}{(1-d_p) + d_p I} \leq 1. \quad (\text{S5})$$

Since $I > 0$, equality in (A8) holds only when $d_p = 0$. Notice that, as the average number of infections per patch (I) increases, r decreases. Notice also that

$$\bar{r}_{(i,j)} = \frac{1}{j} + \frac{j-1}{j} r.$$

The fact that r does not depend on j is worth discussing, since the result may initially appear counterintuitive. The absolute rates of host mortality and local infection within each patch are, of course, in proportion to the number of infected hosts found locally. However, at equilibrium, the impact of each mortality or infection event upon local relatedness is in inverse proportion to the number of local infected hosts. Hence, although relatedness-altering events occur more frequently in patches with more infected hosts, the individual impact of each event is more diluted.

Well-Mixed Pathogen Populations

When pathogen dispersal, $d_p = 1$ we say that the pathogen population is well-mixed. In this case, the class structure of the pathogen population has no bearing on pathogen fitness and pathogens are not related to non-self patchmates. Formally, we can say that $v_{(k,l)} \equiv 1$, $\bar{r}_{(k,l)} = 1/l$, and so

$$\Delta W = -\delta + \delta\beta'(z)S,$$

where $S = \sum_{(i,j)} (i+1)p_{(i+1,j-1)} = \sum_{(i,j)} ip_{(i,j)}$ gives the average number of susceptible

individuals per patch. At evolutionary equilibrium, then, our inclusive fitness model tells us that the marginal fitness benefit due to increased in disease transmission (i.e. the term, $\delta\beta'(z)S$) is exactly balanced by the marginal fitness cost of increased host mortality (i.e. the term, $-\delta$). This same result can be established with a standard game theory model that measures fitness using pathogen lifetime reproductive success, $\beta(z)S/(\mu + z)$ (refs 16,36).

If we assume the simple virulence-transmissibility relationship, $\beta(z) = \beta_{\max} z/(1 + z)$, then disease transmissibility cannot exceed the

maximum level given by β_{\max} . With this assumption it is possible to show that evolution is at equilibrium with respect z when $z = z^* = \sqrt{\mu}$. In particular when $\mu = 1$, $z^* = 1$.

Numerical Investigations

We analyzed the inclusive fitness model from the main text to identify those disease-induced mortality rates associated with the convergence stable levels of host exploitation. Convergence stability is a notion borrowed from evolutionary game theory^{35,37,38}. If z^* is convergence stable, then the distance between z^* and x , the phenotype displayed by successful mutant invaders of a population that is otherwise fixed at z , is always less than the distance between z^* and z . In the context of the present model the disease-induced mortality rate associated with the convergence stable host exploitation rate is an evolutionary equilibrium, z^* that satisfies the following pair of conditions: $\Delta W|_{z=z^*} > 0$ when $\delta < 0$ and $\Delta W|_{z=z^*} < 0$ when $\delta > 0$.

Results were generated through an iterative numerical procedure. For each parameter combination, we began by guessing a corresponding z^* , call it z_0 . Given z_0 , we determined the sign of the inclusive fitness effect, ΔW and refined our guess accordingly. Given the refined guess, z_1 , the sign of ΔW was determined yet again, and further refinements were made. The process of calculating the sign of ΔW and making smaller and smaller refinements continued until successive refinements agreed to several decimal places. We implement our numerical procedure using the computer software package, Maple (version 11).

Predictions made by the inclusive fitness model proposed here agree with those made elsewhere. Most importantly, our model predicts that reduced mixing of the pathogen population (i.e. lower dispersal rate, d_p) promotes reduced host exploitation, and in turn reduced disease-induced host mortality (Figs. S1, S2).

Naturally, the relationship between pathogen mixing and disease-induced host mortality depends on the parameter values under consideration. If there exists a maximum possible transmissibility (β_{\max}), then increasing this maximum encourages larger reductions in disease-induced host mortality (Fig. S1). Moreover, the rate at which such reductions in host mortality occur depend not only β_{\max} but also on N (Fig. S1).

Host reproduction rate (b) and, to a lesser degree, host dispersal rate (d_h) also influence the evolution disease-induced host mortality. Specifically, increasing the value of b and/or d_h reduces the extent to which parasite dispersal influences disease-induced mortality (Fig. S2).

Related Issues

We conclude by clarifying a number of links to existing work. Hamilton³⁹ was the first to suggest that a lower relatedness between the parasites infecting a host would lead to selection for faster exploitation of host resources, and hence a higher virulence. This has since been demonstrated formally by a number of authors^{16,33,40-45}. Our results show that an analogous prediction (albeit more complex) arises in spatially structured populations, where patterns of dispersal determine the relatedness of parasites competing for hosts within patches (see also ref. 33, p.163-168). Our method builds upon previous applications of inclusive fitness theory that have examined the evolution of cooperation³¹ in spatial populations with explicit within and between patch demography. In particular, we follow previous authors by treating the deviant virulence strategy as rare and by neglecting its long-term effects on both patch distribution and reproductive value (see also Appendix A of ref. 32). In this way our analysis focuses on the initial success of a mutant, rather than its probability of fixation. It would certainly be very useful to examine the consequences of demographic stochasticity (e.g. as in ref.

21) or the consequences putting alternative forms of parasite interaction, such as cooperation^{46,47}, or spiteful interference⁴⁸ into an explicit spatial setting (see also ref. 49). Finally, we draw an analogy to the sex ratio literature, where the benefit of determining the underlying selective forces have long been appreciated^{29,50}.

Additional References

31. Alizon, S. & Taylor, P. D. Empty sites can promote altruistic behaviour. *Evolution* **62**, 1335–1344 (2008).
32. Taylor, P. D. & Frank S. A. How to make a kin selection model. *J. Theor. Biol.* **176**, 27–37 (1996).
33. Frank, S. A. *Foundations of Social Evolution*. (Princeton University Press, Princeton, NJ, 1998).
34. Grafen, A. Hamilton's rule OK. *Nature* **318**, 310–311 (1985).
35. Taylor, P. D. Evolutionary stability in one-parameter models under weak selection. *Theor. Popul. Biol.* **36**, 125–143 (1989).
36. Day, T. & Burns, J. G. A consideration of patterns of virulence arising from host-parasite coevolution. *Evolution*, **57**, 671–676 (2003).
37. Eshel, I. Evolutionary and continuous stability. *J. Theor. Biol.* **103**, 99–111 (1983).
38. Christiansen, F. B. On conditions for evolutionary stability for a continuously varying character. *Am. Nat.* **138**, 37–50 (1991).
39. Hamilton, W.D. Altruism and related phenomena, mainly in social insects. *Annu. Rev. Ecol. Syst.* **3**, 193-232 (1972).

40. Bremermann, H. J. & Pickering, J. A game-theoretical model of parasite virulence. *J. Theor. Biol.* **100**, 411-26 (1983).
41. Frank, S. A. Kin selection and virulence in the evolution of protocells and parasites. *Proc. Roy. Soc. Lond. B* **258**, 153-61 (1994).
42. Nowak, M. & May, R. M. Superinfection and the evolution of parasite virulence. *Proc. Roy. Soc. Lond. B* **255**, 81-89 (1994).
43. May, R. M. & Nowak, M. A. Coinfection and the evolution of parasite virulence." *Proc. R. Soc. Lond. B* **261**, 209-15 (1995).
44. van Baalen, M. & Sabelis M. W. The dynamics of multiple infection and the evolution of virulence. *Am. Nat.* **146**, 881-910 (1995).
45. Gandon, S. & Michalakis, Y. Evolution of parasite virulence against qualitative or quantitative host resistance. *Proc. Roy. Soc. Lond. B* **267**, 985-990 (2000).
46. Brown, S. P., Hochberg, M. E. & Grenfell, B. T. Does multiple infection select for raised virulence? *Trends in Microbiology* **10**, 401-405 (2002).
47. West, S. A. & Buckling, A. Cooperation, virulence and siderophore production in bacterial parasites. *Proc. Roy. Soc. Lond. B* **270**, pp. 37-44 (2003).
48. Gardner, A., West, S. A. & Buckling, A. Bacteriocins, spite and virulence." *Proc. Roy. Soc. Lond. B* **271**, 1529-2535 (2004).
49. Lion, S. & Gandon, S. Habitat saturation and the spatial evolutionary ecology of altruism. *J. Evol. Biol.*, in press.
50. Taylor, P D. Intra-sex and inter-sex sibling interactions as sex determinants. *Nature* **291**, 64-66 (1981).

Table S1. Rates $q_{(i,j),(k,l)}$ (from eqn S1) at which class- (i,j) patches are (a) created and (b) destroyed. Recall that i and j denote the number of susceptible and infected hosts, respectively, found on a given patch. We assume $i, j \geq 0$, with $i + j \leq N$

$(k,l) \rightarrow (i,j)$	Description	$q_{(i,j),(k,l)}$
(a) Inputs to class- (i,j)		
$(i+1,j) \rightarrow (i,j)$	susceptible host dies on $(i+1,j)$ -patch	$\mu(i+1)$ (or zero if $i+j=N$)
$(i-1,j) \rightarrow (i,j)$	newborn host arrives on $(i-1,j)$ -patch	$b_{(i-1,j)}$
$(i,j+1) \rightarrow (i,j)$	infected host dies on $(i,j+1)$ -patch	$(\mu+z)(j+1)$ (or zero if $i+j=N$)
$(i+1,j-1) \rightarrow (i,j)$	infection occurs on $(i+1,j-1)$ -patch	$\beta_{(i+1,j-1)}(z)$
(b) Outputs from class- (i,j)		
$(i,j) \rightarrow (i-1,j)$	susceptible host dies on (i,j) -patch	μi
$(i,j) \rightarrow (i+1,j)$	newborn host arrives on (i,j) -patch	$b_{(i,j)}$
$(i,j) \rightarrow (i,j-1)$	infected host dies on (i,j) -patch	$(\mu+z)j$
$(i,j) \rightarrow (i-1,j+1)$	infection occurs on (i,j) -patch	$\beta_{(i,j)}(z)$

Table S2. Expressions for wild-type, or “normal” fitness function, $w_{(i,j),(k,l)}$. Recall that $j, l \geq 1$ when describing pathogen class structure.

(i,j)	$w_{(i,j),(k,l)}$
(k, l)	$-(\mu k + (\mu + z)l + b_{(k,l)} + \beta_{(k,l)}(z)) + \tilde{\beta}_{(k,l)}(z)$
$(k-1, l)$	$\mu k + \tilde{\beta}_{(k-1,l)}(z)$
$(k+1, l)$	$b_{(k,l)} + \tilde{\beta}_{(k+1,l)}(z)$
$(k, l-1)$	$(\mu + z)(l-1) + \tilde{\beta}_{(k,l-1)}(z)$
$(k-1, l+1)$	$\beta(z)(1-d_p)k + \beta_{(k,l)}(z) + \tilde{\beta}_{(k-1,l+1)}(z)$
all others	$\tilde{\beta}_{(i,j)}(z)$

Figure Legends

Fig. S1. Relationship between stable level of disease-induced host mortality (i.e. ES virulence, z^*) and pathogen dispersal rate, d_p as both patch carrying capacity (N) and maximum disease transmissibility ($\beta_{\max} = \lim_{x \rightarrow \infty} \beta(x)$) vary. Remaining parameters were $\mu = 1$, $d_h = 0.3$ and $b = 3$, and $\beta(x)$ was assumed to take the form, $\beta_{\max} x/(1+x)$ (see text for parameter definitions). From top to bottom $\beta_{\max} = 5, 7.5$, and 20 , respectively. Results for additional values of β_{\max} are presented as dashed lines (values are as indicated). The qualitative pattern illustrated in panels corresponding to $N = 3, 5$ was also identified for $N = 10$, however the effect was too small to be seen easily along side other plots.

Fig. S2. Relationship between stable level of disease-induced host mortality (i.e. ES virulence, z^*) and pathogen dispersal rate, d_p as both patch carrying capacity (N) and host life-history parameters vary. Remaining parameters were $\mu = 1$ and $\beta(x) = 5x/(1+x)$ (see text for definitions). (a) From top to bottom host dispersal takes values $d_h = 0.9, 0.6$, and 0.3 respectively under the assumption that $b = 3$. (b) From top to bottom host dispersal takes values $b = 9, 6$, and 3 respectively under the assumption that $d_h = 0.3$. Results for additional values of b are presented as dashed lines in (b) (values are as indicated). To better elucidate the effect of changes in host life-history parameters for the case $N = 2$, numerical analyses were also carried out assuming $\beta(x) = 15x/(1+x)$. These additional results are presented as inset figures whose axes display the same range of d_p and z^* values used in the main panels.

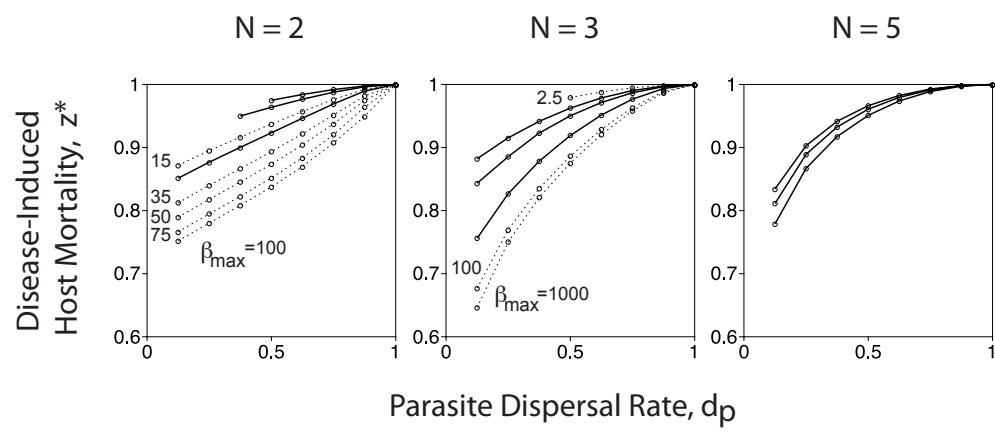


Fig. S1

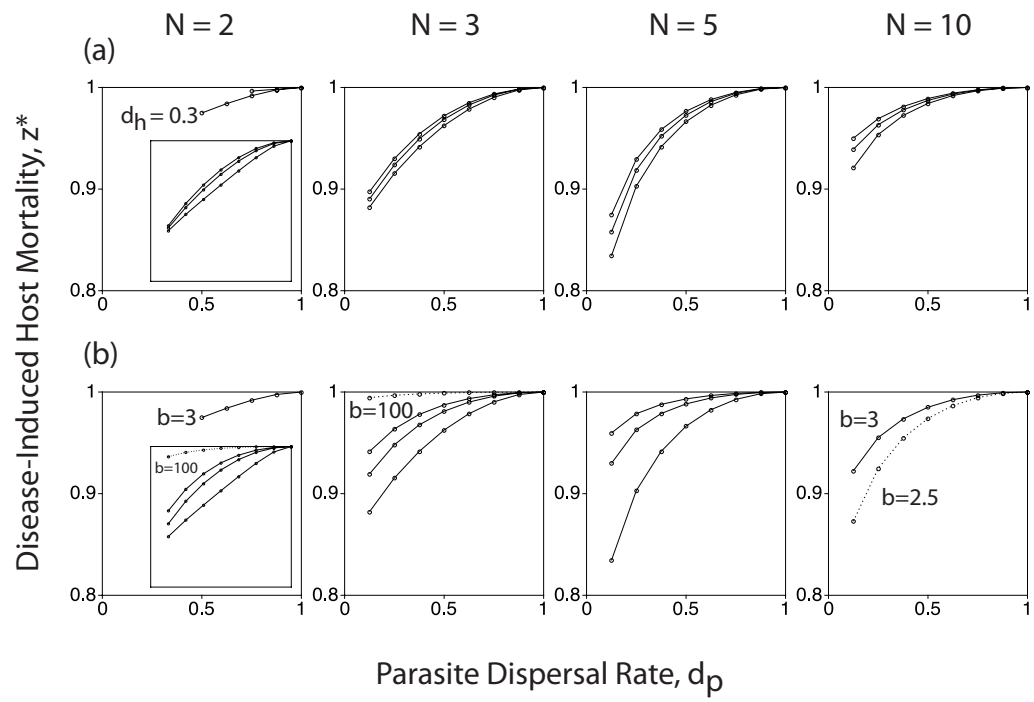


Fig. S2